Nuclear Science and Techniques **24** (2013) 050522

Interferometry signatures of hydrodynamic sources with fluctuating initial conditions

HU Ying SU Zhongqian ZHANG Weining*

School of Physics and Optoelectronic Technology, Dalian University of Technology, Dalian 116024, China

Abstract We investigate the space-time evolution of the hydrodynamic particle-emitting sources with the fluctuating initial conditions generated by Heavy Ion Jet Interaction Generator (HIJING). In order to detect the event-by-event inhomogeneity of the sources, we examine the distribution of the error-inverse-weighted fluctuations, f, between the two-pion Bose-Einstein correlation functions of single and mixed events. We find that the distribution of f becomes wide for the fluctuating initial conditions. The large values of the distribution width and the root-mean-square f_{rms} are the signatures of the hydrodynamic particle-emitting sources with the fluctuating initial conditions.

Key words Hydrodynamic source, Fluctuating initial condition, Interferometry signature, Event-by-event analysis

1 Introduction

Relativistic hydrodynamics has been widely used to describe the system evolution in high energy heavy ion collisions[1–3]. It provides the link between the initial and final states of the systems produced in the collisions. In general, the initial systems produced in relativistic heavy ion collisions are not spatially uniform, and there are event-by-event fluctuations of the initial quantities[4]. These initial fluctuations may affect the system evolution of space-time and lead to some changes of final particle observables relative to those associated with smoothed initial conditions[4–8].

Hanbury-Brown-Twiss (HBT) interferometry is a useful tool for probing the space-time structure of the particle-emitting sources in high energy heavy ion collisions[9–12]. Previous studies indicate that the single event HBT correlation functions of the final identical pions exhibit event-by-event fluctuations in the granular source model[13,14] and Smoothed Particle Hydrodynamics (SPH) model[15]. Investigating the propagation of the initial fluctuations through system evolution and detecting their effects on the HBT measurements in relativistic heavy ion collisions are interesting issues. In this work, we use the Heavy Ion Jet Interaction Generator (HIJING)[16] to generate the initial states of the systems event-by-event, at the energies of the Relativistic Heavy Ion Collider (RHIC) and the Large Hadron Collider (LHC). Then, we model the evolution of the particle-emitting sources with a (2+1) dimension relativistic hydrodynamics with the fluctuating initial conditions. Using the HBT technique based on event-by-event analysis[14,15], we investigate the effect of the fluctuating initial conditions on the space-time evolution of the particle-emitting sources. It is found that the particle-emitting sources with HIJING fluctuating initial conditions are inhomogeneous in space. The single-event two-pion correlation functions for the inhomogeneous sources exhibit event-by-event fluctuations. The large width of the distribution of the error-inverse-weighted fluctuations, f, between the correlation functions of single and mixed events, and the large values of the root-mean-square f_{rms} are the signatures of the particle-emitting sources with the fluctuating initial conditions.

2 Hydrodynamic evolution of the systems with fluctuating initial conditions

In the heavy ion collisions at RHIC and LHC energies,

Supported by National Natural Science Foundation of China (NSFC) projects (Nos.11075027 and 11275037).

* Corresponding author. *E-mail address:* wnzhang@dlut.edu.cn

Received date: 2013-06-27

the net baryon density of system is about zero because of the collision transparence. The ideal hydrodynamic description for the system with zero net baryon density is defined only by local energy and momentum conservation[1,2]. Under the assumption of Bjorken longitudinal boost invariance[17], the hydrodynamics in (3+1) dimension reduces to a (2+1) dimension hydrodynamics, and we need only to solve the transverse (*xy*-plane) equations of motion[18]. Assuming that the system achieves local equilibrium at time τ_0, we can use HIJING to construct the event-by-event initial energy density of the hydrodynamic evolving source at *z*=0 as[19,20]

$$\varepsilon(\tau_0, x, y, z=0) = K\sum_{\alpha}\frac{p_{\perp\alpha}}{\tau_0}\frac{1}{2\pi\sigma_{\perp}^2} \times \exp\left\{-\frac{[x-x_\alpha(\tau_0)]^2+[y-y_\alpha(\tau_0)]^2}{2\sigma_{\perp}^2}\right\}, \tag{1}$$

where $p_{\perp\alpha}$ is the transverse momentum of parton α, $x_\alpha(\tau_0)$ and $y_\alpha(\tau_0)$ are the transverse coordinates of the parton at τ_0, $\sigma_\perp$ is a transverse width parameter and K is a scale factor which can be adjusted to fit the experimental data of produced hadrons.

Figure 1 shows the initial transverse distributions of two single events constructed with the HIJING at $\tau_0 = 0.6$ fm/*c* for $\sqrt{s_{NN}} = 200$ GeV Au+Au collisions with impact parameter *b*=4 fm and 8 fm, respectively. The parameters $\sigma_\perp$ and K are taken to be 0.5 fm and 0.8. One can see clearly that the transverse distribution of energy density for each event has large fluctuation, which leads to some "hot spots" in the initial sources. The number and maximum values of the spots decrease with the increase of impact parameter.

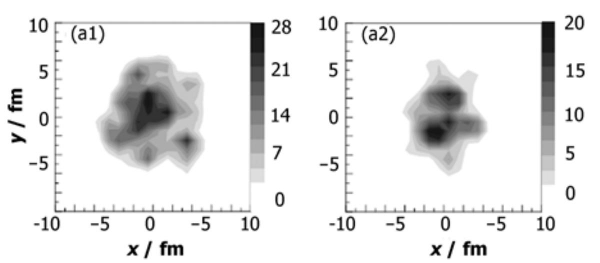

Fig.1 Initial transverse distributions of energy density of two single events for Au+Au collisions at $\sqrt{s_{NN}} = 200$ GeV, constructed with the HIJING at $\tau_0 = 0.6$ fm/*c*. The panel (a1) is for the impact parameter $b=4$ fm and the panel (a2) is for $b=8$ fm. The unit of energy density is GeV/fm^3.

To solve the hydrodynamic equations of motion, we also need the equation of state (EOS) which closes the hydrodynamic equations. In the calculations, we use the parameterized EOS named s95p-PCE[21], which combines the hadron resonance gas at low temperature and the lattice QCD results at high temperature.

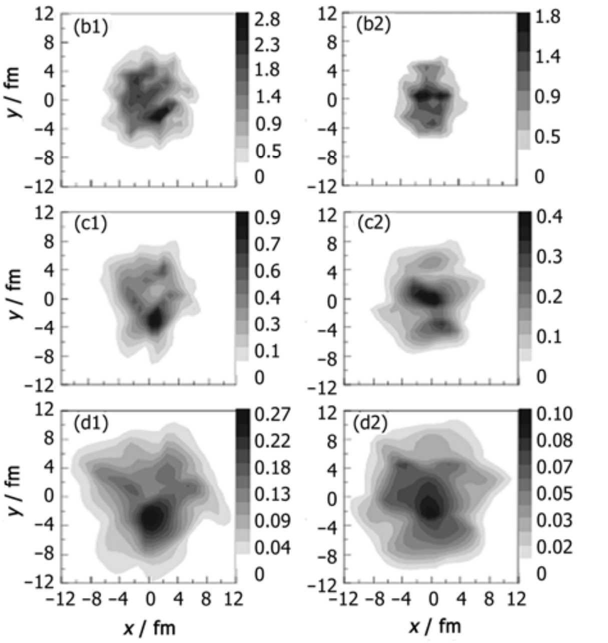

Fig.2 Transverse distributions of energy density of the two single events with $b=4$ fm (left panels) and 8 fm (right panels), at $z=0$ and $t=3$ fm/*c* [(b1) and (b2)], $t=6$ fm/*c* [(c1) and (c2)], and $t=9$ fm/*c* [(d1) and (d2)]. The initial conditions for panels (b1)–(d1) and (b2)–(d2) are the same as in Fig.1(a1) and (a2), respectively. The unit of energy density is Gev/fm^3.

Once the initial conditions and EOS are determined, we can solve the hydrodynamic equations numerically. Figs.2(b1)–(d1) and (b2)–(d2) show the solutions of the transverse distributions of energy density at *z*=0 and *t*=3, 6, and 9 fm/*c*, for the two single-event sources with the HIJING initial conditions present in Figs.1(a1) and (a2), respectively. In the calculations, we ues the HLLE scheme[1,22] and the Sod's operator splitting method[1,22,23] to solve the hydrodynamic equations in the transverse plane *z*=0, and obtain the hydrodynamic solutions at *z*≠0 by the longitudinal boost invariance of Bjorken hypothesis[17,18]. The grid sizes for the HLLE is taken to be $\Delta x = \Delta y = 0.1$ fm, and the time step is taken to be $\Delta t = 0.99 \cdot \Delta x$ for the Courant-Friedrichs-Lewy (CFL) criterion, $\Delta t / \Delta x = \nu < 1$ [1,22]. From Fig.2 it can be seen that the transverse distributions of the energy density have large event-by-event fluctuations in space.

These fluctuations are reserved even at the late stage of the evolution at t=9 fm/c.

3 HBT signatures of inhomogeneous particle-emitting sources

The HBT correlation function of identical pions is defined as the ratio of the two-pion momentum distribution $P(\vec{p}_1, \vec{p}_2)$ to the product of the single-pion momentum distribution $P(\vec{p}_1)P(\vec{p}_2)$. Assuming that final identical pions are emitted at the space-time configuration characterized by a freeze-out temperature T_f, we can generate the pion momentum $\vec{p}_i\ (i=1,2)$ according to Bose-Einstein distribution, and then construct the single-event and mixed-event two-pion correlation functions[5,14].

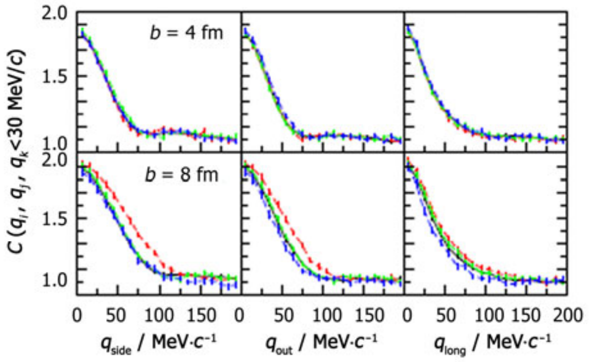

Fig.3 (Color online) Two-pion correlation functions for different single events (dashed lines) and mixed events (solid lines) with impact parameters b=4 fm (up panels) and b=8 fm (down panels).

In Fig.3, we show our model-calculated two-pion correlation functions, C ($q_{\rm side}$, $q_{\rm out}$, $q_{\rm long}$), for the single and mixed events with the HIJING initial conditions for $\sqrt{s_{NN}}$ = 200 GeV Au+Au collisions with $b=4$ fm (up panels) and b=8 fm (down panels). Here the variables $q_{\rm side}$, $q_{\rm out}$, and $q_{\rm long}$ are the components of "side", "out", and "long" of relative momentum of pion pair[24,25]. The dash lines in each panel are the results for three different single events and the solid line is for the mixed event constructed with 80 single events. In the calculations, the freeze-out temperature is taken to be 120 MeV, and the total number of correlated pion-pairs in each event is $N_{\pi\pi}$=10^6. One can see from Fig.3 that the correlation functions for the single events exhibit fluctuations relative to those for the mixed events, especially for the bigger impact parameter. This is because that the smaller number of the hot spots in the system with larger impact parameter may increase the source granularity[6,7], and lead to larger fluctuations[6,7]. However, in the usual mixed-event HBT analysis, these event-by-event fluctuations of single-event two-pion correlation functions are smoothed out.

In order to observe the event-by-event fluctuations, we investigate the ratio of signal to noise of the fluctuations between the correlation functions of single and mixed events $|C_{\rm s}(q_i)-C_{\rm m}(q_i)|$[14,15],

$$f(q_i)=\frac{|C_{\rm s}(q_i)-C_{\rm m}(q_i)|}{\Delta|C_{\rm s}(q_i)-C_{\rm m}(q_i)|}, \qquad (2)$$

where i is the index of the component of relative momentum q, and $\Delta|C_{\rm s}(q_i)-C_{\rm m}(q_i)|$ is the error of the fluctuation.

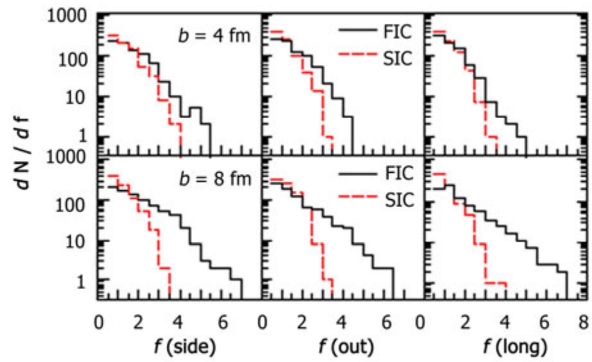

Fig.4 (Color online) Distributions dN/df for 80 FIC and SIC events with impact parameters $b=4$ fm (up panels) and $b=8$ fm (down panels). $N_{\pi\pi}$=10^6.

In Fig.4, we show the distributions of dN/df in the side, out, and long directions obtained from the 80 events with impact parameter b=4 and 8, respectively. In calculations we take the width of the relative momentum q_i bin to be 10 MeV/c and use the bins in the region $20\le q_i \le 200$ MeV/c. The number of correlated pion pairs for each event is taken to be $N_{\pi\pi}$=10^6. In Fig.4, the solid lines are the results for the fluctuating initial conditions (FIC). For comparison, the corresponding distributions for the events with the smoothed initial conditions (SIC), which are obtained by averaging over 400 random HIJING events, are shown with the dashed lines. One can see that the f distributions for FIC are wider than the corresponding results for SIC. The widths of the distributions for FIC increase with impact parameter. But the widths of the distributions for SIC are small and almost invariant with the increase of impact parameter. This is because

that the fluctuations of the single-event correlation functions for SIC are small always.

For a limited $N_{\pi\pi}$, we can reduce the number of analysis variable to decrease the noise in Eq.(2) and increase the ratio of signal to noise f, although it may lose some details. In Fig.5 we show the distributions of the f calculated with the variables of transverse relative momentum q_T [panels (a) and (b)] and relative momentum q [panels (c) and (d)] of the pion pairs. The impact parameter b is 8 fm. One can see that the widths of the distributions of f for FIC increase with the number of the pion pairs in an event, $N_{\pi\pi}$. Even for $N_{\pi\pi}=10^5$, the widths for FIC are visibly larger than those for SIC.

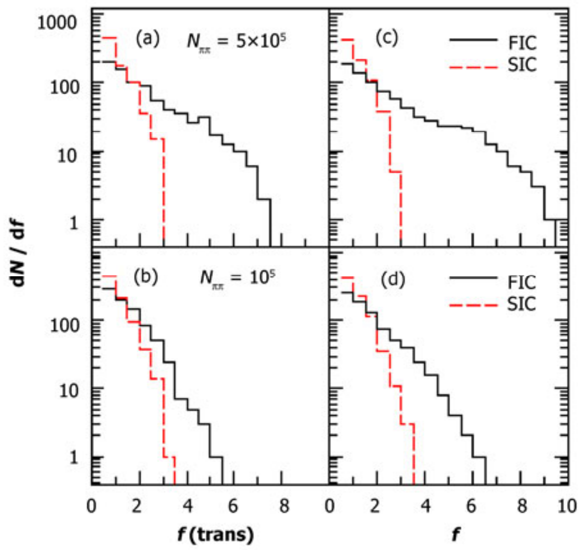

Fig.5 (Color online) Distributions dN/df for 80 FIC and SIC events with impact parameters $b = 8$ fm, where f are calculated for variables q_T [(a) and (b)] and q [(c) and (d)].

Next we examine quantitatively the widths of the distributions, dN/df, for the relativistic heavy ion collisions at RHIC and LHC energies. In Fig.6, we show the root-mean-square (RMS) of f as a function of $N_{\pi\pi}$ calculated from the 40 simulated events for Au+Au collisions at $\sqrt{s_{NN}}$ = 200 GeV and Pb+Pb collisions at $\sqrt{s_{NN}}$ = 2.76 TeV, respectively.

From Fig.6 we can see that the values of $f_{\rm rms}$ for FIC increase with $N_{\pi\pi}$. But for SIC the values of $f_{\rm rms}$ are almost independent of $N_{\pi\pi}$. The reason is that for FIC the errors in Eq.(2) decrease with $N_{\pi\pi}$ and for SIC both the differences $|C_{\rm s}(q) - C_{\rm m}(q)|$ and their errors decrease with $N_{\pi\pi}$. For the larger impact parameter, the $f_{\rm rms}$ for FIC increase more rapidly with $N_{\pi\pi}$ because the number of the hot spots is smaller in this case. At LHC energy, we find that the hot-spot number in the source is larger than that at RHIC energy and with the same impact parameter. This leads to the smaller $f_{\rm rms}$ for FIC at LHC energy as compared to that at RHIC energy.

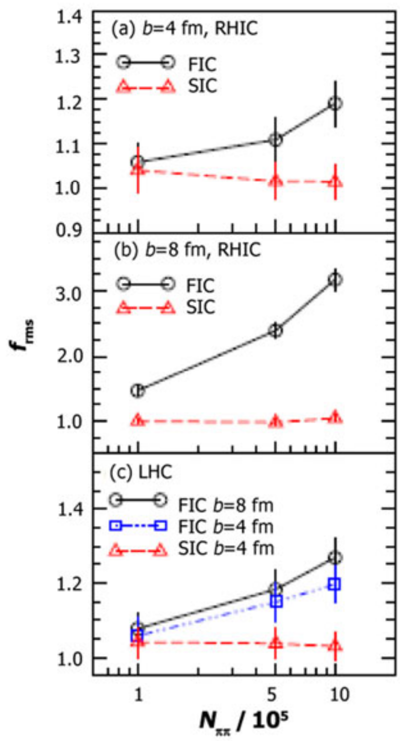

Fig.6 (Color online) Root-mean-square of f as a function of $N_{\pi\pi}$ for the heavy ion collisions at RHIC and LHC energies.

In experiments the number of correlated pion pairs in one event, $N_{\pi\pi}$, is limited. For the central collisions at RHIC energy, the event multiplicity of identical pion, M_π, is about several hundreds and $N_{\pi\pi}$ is about 10^5 ($\sim M_\pi^2/2$). However, at LHC energy, M_π is about several thousands and $N_{\pi\pi}$ may reach to 10^6. From Fig. 6 one can see that in these cases the results of $f_{\rm rms}$ for FIC are visibly larger than those for SIC. The signatures of dN/df and $f_{\rm rms}$ for the inhomogeneous particle-emitting sources are hopefully to be detected in the heavy ion collisions at RHIC and LHC.

4 Conclusion

Using the hydrodynamic model with HIJING event-by-event fluctuating initial conditions, we investigate the space-time evolution of the particle-emitting sources in relativistic heavy ion collisions. The results indicate that the fluctuating

initial conditions may lead to event-by-event inhomogeneous particle-emitting sources. For these inhomogeneous sources the single-event two-pion correlation functions exhibit large fluctuations. However, in the usual HBT analyses performed for mixed events, these event-by-event fluctuations of the single-event correlation functions are smoothed out.

In order to observe the fluctuations of the correlation functions, we investigate the distributions of f, the fluctuations between the two-pion correlation functions of single and mixed events with their error-inverse weights. We find that the widths of the distributions dN/df for FIC are much wider than those for SIC. Correspondingly, the values of the root-mean-square $f_{\rm rms}$ for FIC are larger. For FIC, $f_{\rm rms}$ increases with the impact parameter of collisions, because the smaller number of the hot spots in the system with larger impact parameter may lead to a larger source granularity. The values of $f_{\rm rms}$ for FIC increase with the number of correlated pion pairs, $N_{\pi\pi}$. However, the values of $f_{\rm rms}$ for SIC are almost independent of $N_{\pi\pi}$. The large values of the distribution width and the root-mean-square $f_{\rm rms}$ are the signatures of the particle-emitting source with the fluctuating initial conditions. Our calculations indicate that these signatures are hopefully to be detected in the heavy ion collisions at RHIC and LHC.

References

1 Rischke D H. arXiv:nucl-th/9809044.

2 Kolb P F and Heinz U. arXiv:nucl-th/0305084.

3 Ollitraulta J Y, Gardimbar F G. arXiv:1210.8345[nucl-th].

4 Adare A, Luzum M, Petersen H. arXiv: 1212.5388 [nucl-th].

5 Zhang W N, Ren Y Y, Wong C Y. Phys Rev C, 2006, **74:** 024908.

6 Yang Z T, Zhang W N, Huo L, *et al.* J Phys G, 2009, **36:** 015113.

7 Zhang W N, Yang Z T, Ren Y Y. Phys Rev C, 2009, **80:** 044908.

8 Zhang W N, Yin H J, Ren Y Y. Chin Phys Lett, 2011, **28:** 122501.

9 Wong C Y. Introduction to High-Energy Heavy-Ion Collisions (chap 17). Singapore: World Scientific, 1994.

10 Wiedemann U A and Heinz U. Phys Rep, 1999, **319:** 145–230.

11 Weiner R M. Phys Rep, **327:** 249–346.

12 Lisa M A, Pratt S, Soltz R, Wiedemann U. Ann Rev Nucl Part Sci, 2005, **55:** 357–402.

13 Wong C Y and Zhang W N. Phys Rev C, 2004, **70:** 064904.

14 Zhang W N, Li S X, Wong C Y, *et al.* Phys Rev C, 2005, **71:** 064908.

15 Ren Y Y, Zhang W N, Liu J L. Phys Lett B, 2008, **669:** 317–320.

16 Wang X N. Phys Rep, 1997, **280:** 287–371.

17 Bjorken J D. Phys Rev D, 1983, **27:** 140–151.

18 Baym G, Friman B L, Blazot J P, *et al.* Nucl Phys A, 1983, **407:** 541–570.

19 Guylassy M, Rischke D H, Zhang B. Nucl Phys A, 1997, **613:** 397–434.

20 Pang L G, Wang Q, Wang X N. Phys Rev C, 2012, **86:** 024911.

21 Shen Chum, Heinz U, Huovinen P, *et al*. Phys Rev C, 2010, **82:** 054904.

22 Rischke D H and Gyulassy M. Nucl Phys A, 1996, **608:** 479–512.

23 Sod G A. J Fluid Mech, 1977, **83:** 785.

24 Bertsch G, Gong M, Tohyama M. Phys Rev C, 1988, **37:** 1896–1900.

25 Pratt S, Csorgo T, Zimanyi J. Phys Rev C, 1990, **42:** 2646–2652.